Surface-interface exploration of Mg deposited on Si(100) and oxidation effect on interfacial layer

S Sarpi, Rachid Daineche, Christophe Girardeaux, M Bertoglio, F Derivaux, J P Biberian, Anne Hémeryck, S Vizzini

Surface-interface exploration of Mg deposited on Si(100) and oxidation effect on interfacial layer

B. Sarpi, R. Daineche, C. Girardeaux, M. Bertoglio, F. Derivaux, J. P. Biberian, A. Hemeryck, and S. Vizzini

Citation: Applied Physics Letters **106**, 021604 (2015); doi: 10.1063/1.4905592
View online: http://dx.doi.org/10.1063/1.4905592
View Table of Contents: http://scitation.aip.org/content/aip/journal/apl/106/2?ver=pdfcov
Published by the AIP Publishing

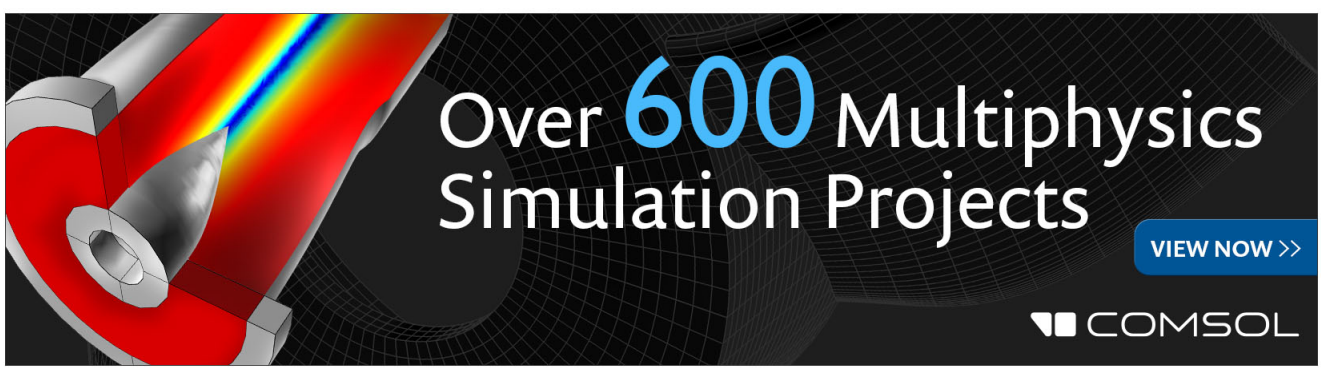

Surface-interface exploration of Mg deposited on Si(100) and oxidation effect on interfacial layer

B. Sarpi,[1] R. Daineche,[1] C. Girardeaux,[1] M. Bertoglio,[1] F. Derivaux,[1] J. P. Biberian,[2] A. Hemeryck,[3,4] and S. Vizzini[1,a)]
[1]*Aix Marseille Univ, IM2NP, Fac Sci St Jérôme, F-13397 Marseille, France*
[2]*Aix Marseille Univ, CINaM CNRS, F-13288 Marseille, France*
[3]*CNRS, LAAS, 7 Avenue du Colonel Roche, F-31400 Toulouse, France*
[4]*Univ de Toulouse, LAAS, F-31400 Toulouse, France*

(Received 21 July 2014; accepted 26 December 2014; published online 14 January 2015)

Using scanning tunneling microscopy and spectroscopy, Auger electron spectroscopy, and low energy electron diffraction, we have studied the growth of Mg deposited on Si(100)-(2 × 1). Coverage from 0.05 monolayer (ML) to 3 ML was investigated at room temperature. The growth mode of the magnesium is a two steps process. At very low coverage, there is formation of an amorphous ultrathin silicide layer with a band gap of 0.74 eV, followed by a layer-by-layer growth of Mg on top of this silicide layer. Topographic images reveal that each metallic Mg layer is formed by 2D islands coalescence process on top of the silicide interfacial layer. During oxidation of the Mg monolayer, the interfacial silicide layer acts as diffusion barrier for the oxygen atoms with a decomposition of the silicide film to a magnesium oxide as function of O_2 exposure. © *2015 AIP Publishing LLC*. [http://dx.doi.org/10.1063/1.4905592]

The controlled growth of ultrathin oxide films is of crucial importance for technological applications in microelectronics[1] and particularly in semiconductor-based spintronic.[2] The main issue is to find new routes to process well controlled homogenous oxide layers on semiconductor surfaces known for their high reactivity to oxygen species, and more precisely on how to reach a high-quality interface between the deposit and the silicon substrate.[3–5] Some recent studies explore an innovating growth method, in which the oxidation is performed at room temperature (RT) on a metallic monolayer (ML) previously deposited on silver or silicon substrates[6–11] resulting in a high homogenous oxide layer, with sharp interfaces and preventing oxidation of the silicon substrate. To master this process, it is crucial to finely control and get a fundamental description with an atomic scale precision about the deposition of the metallic layer in direct contact with the substrate.

Mg on Si(100) has been investigated by several groups,[12–16] due to the great interest in low work function metal-on-semiconductor systems for technological application as efficient photocathodes or as thermionic energy converters.[17,18] While scanning tunneling microscopy (STM) works of Mg on Si(100)[12,16] were limited to 0.25 ML, we focused our studies up to 3 ML.

We have shown the formation of a Mg_2Si ultra-thin silicide layer at the interface. We also studied the oxidation of one Mg ML and highlighted a strong effect on this interfacial layer. Note the great interest of thin silicide properties as Mg_2Si for thermoelectric applications[19] or MgB_2 superconducting thin films on Si(100).[20] Here, the choice of Mg is motivated by the high potentiality of its oxide as an insulating barrier for magnetic tunnel junctions[21,22] and silicon-based spintronics.[2]

All experiments were performed in an ultra-high vacuum (UHV) chamber equipped with a commercial Omicron variable temperature-scanning tunneling microscopy, an Omicron Spectra-low energy electron diffraction (LEED), and a Riber CMA Auger spectrometer. The Si(100) sample was outgassed at 700 °C over night, flashed briefly to 1100 °C, and then cooled slowly (50 °C/3 min) from 900 °C to 650 °C. This procedure was reiterated until a sharp (2 × 1) LEED pattern and organized Si dimer rows characteristic of a reconstructed Si(100) surface was obtained by STM. Mg was deposited *in situ* at RT from a calibrated effusion cell in the 10^{-10} Torr range. The deposition rate was calibrated using Auger electron spectroscopy (AES) in a derivate mode and compared with other calibrations using quartz crystals (in the following discussion, 1 ML = 7.88 × 10^{14} atoms/cm^2, atomic density of the Si(100) surface layer). The oxidation process of one Mg monolayer was performed at RT by exposing the sample to a constant pressure of molecular oxygen (1×10^{-8} Torr) in the chamber.

Figure 1(a) presents the evolution of the normalized peak-to-peak Auger intensities of the Si_(92 eV) substrate and the Mg_(45 eV) adsorbate versus deposition time. A continuous variation appears for both substrate and adsorbate intensities until constant values (close to 0 for silicon and close to 1 for Mg) are reached. From the shape of the curves, one can deduce the growth mode mechanism.[23] A logarithmic representation of the Auger Si_(92 eV) signal versus deposition time is given in Figure 1(b), where a nearly linear decay corresponding to an exponential attenuation of the substrate intensity is observed. This reveals a layer-by-layer growth mode for Mg at RT[24] where each break on the curves corresponds to a monolayer completion (highlighted by vertical lines on Figure 1(a)).

Additional STM investigations detailed hereafter enable to identify two different modes in addition to the Auger curves: one corresponding to an underlayer completion close to 0.25 ML (Figure 1, dashed line) and a second one related

a)Author to whom correspondence should be addressed. Electronic mail: sebastien.vizzini@im2np.fr.

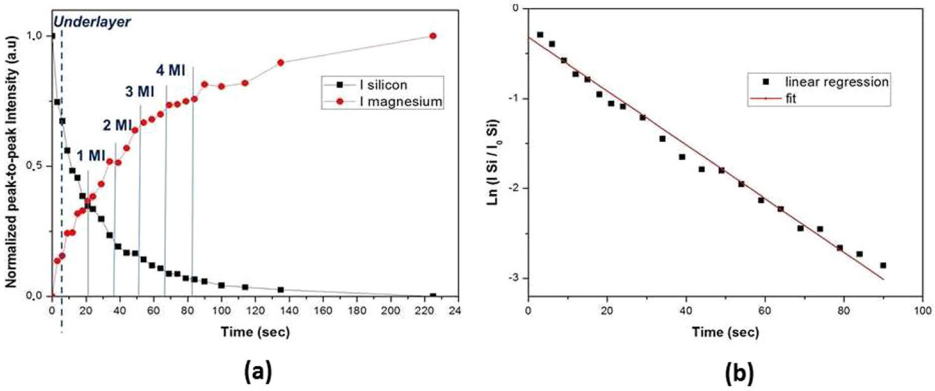

FIG. 1. (a) Peak-to-peak Auger signals as a function of time during the deposition of Mg on Si(100) at RT. (b) Logarithmic representation of the Auger Silicon (black squares) and best linear fit (red line). The dashed line corresponds to the formation of the silicide underlayer observed by STM.

to the layer-by-layer growth of Mg atoms on top of this underlayer. The formation of the underlayer was predicted by van Buuren *et al.* by X-ray photoelectron spectroscopy (XPS) showing Mg core-level data as a function of Mg coverage[14] and attributed to a thin silicide layer of Mg_2Si.

It is reasonable to assume that one Mg ML corresponds in Figure 1(a) to the first break observed on the Si and Mg signals after 21 s of deposition (as expected for a layer-by-layer growth mode). So that, it is possible to evaluate the Mg/Si intensities ratio obtained for each successive monolayer. After 1 ML of deposition, the silicon Auger peak is attenuated by about 54% of its initial value.

Using the attenuation equations,[25,26] we deduce from the AES the Mg thickness obtained after 1 ML of deposition (2.7 Å), in agreement with the Mg atomic diameter of 2.9 Å.

As metal deposition increases, the LEED (2 × 1) reconstruction pattern gradually fades away and disappears completely at 0.3 ML of Mg coverage, in agreement with the previous studies.[12] As more Mg is deposited, Mg specie has disrupted the surface and removed the long-range order associated with the Si(100)-(2 × 1) surface reconstruction as shown by LEED as a disordered surface.

Note that at low coverage, 2 × 2 and 2 × 3 Mg reconstructions were reported by Kubo *et al.*,[16] formed by thermal desorption of Mg. This is in agreement with earlier AES-LEED experiments performed by Kawashima *et al.*[13]

The growth at extremely low coverage of Mg on well-defined Si(100)-(2 × 1) was explored. Figure 2(a) displays a typical topographic empty state STM image of the reconstructed Si(100)-(2 × 1) surface characterized by typical rows of silicon dimers. Figure 2(b) presents an empty state STM image of the Si(100)-(2 × 1) surface after deposition of about 0.05 ML of Mg. Note that the deposition time corresponding to the first break on Figure 1(a) was divided by 20 to reach 0.05 ML coverage rate. An inset area enlargement is given in Figure 2(c). In this image, the blue line corresponds to the height profile drawn in Figure 2(d). The Mg adatoms that appear as the brightest features are approximately 70 pm high and may induce a large amount of buckling in the Si dimers near the Mg rows as presented in Figure 2(c). Some Si dimer rows are still uncovered and Mg atoms preferentially organized in rows that run mainly perpendicular to the dimer rows. These Mg features observations at the early stages of growth are consistent with the study carried out by

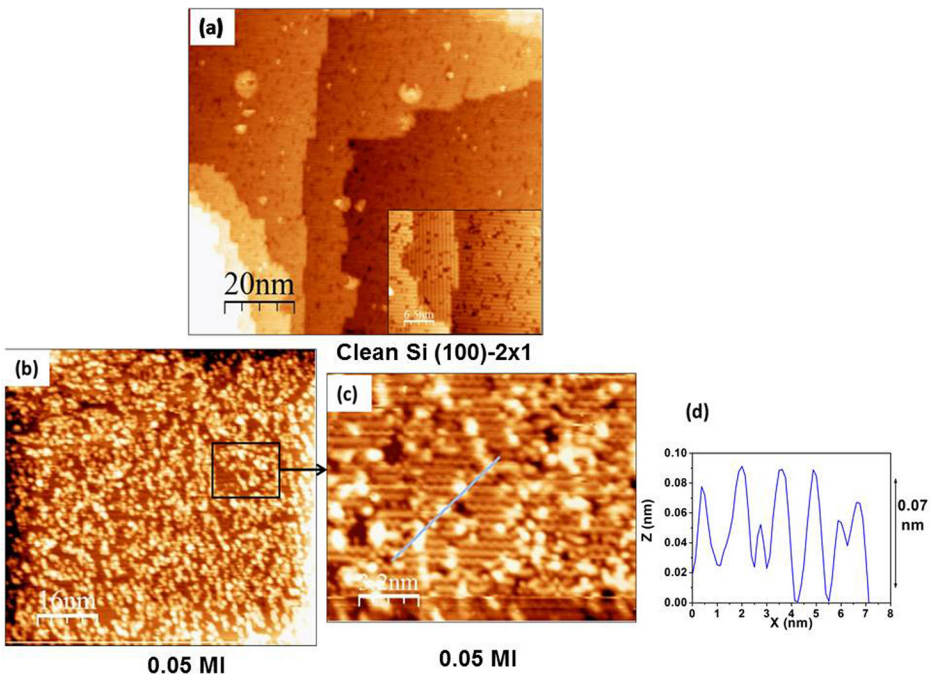

FIG. 2. (a) 100 × 100 nm^2 empty state STM image of the reconstructed Si(100)-(2 × 1) clean surface (V = −1.9 V). (b) 80 × 80 nm^2 empty state STM image recorded after 0.05 ML of Mg deposition (V = −2 V). (c) 15 × 15 nm^2 empty state STM image focused on the inset area of (b) (V = −2 V). (d) Height profile corresponding to the blue line drawn on (c).

Hutchinson *et al.*[12] and Kubo *et al.*[16] for coverages under 0.2 ML and further corroborate their deposition calibration performed using quartz crystal balance and STM.

Increasing the Mg coverage, we report in Figure 3(a) an empty state STM image recorded after around 0.25 ML of deposition. At this deposition level, the silicon surface seems already saturated by Mg adatoms.

This can be explained by preferential adsorption sites for Mg onto the reconstructed Si(100)-(2 × 1) surface, as discussed by Hutchinson *et al.*[12]

As observed in Figure 3(a), the deposition of about 0.25 Mg ML leads to the formation of a complete underlayer resulting of a distinctive 70 pm high topography on the covered substrate. From their morphology, we can reasonably assume that these Mg features are similar to the ones previously observed in the early stages of growth (Figure 2(b)). However, the larger density leads to an entire coverage of the silicon surface. Note that from very sharped step edges observed on clean silicon surfaces results to un-sharped step edges and rough surface characteristic of a disordered surface alloy consistent with extinguished LEED pattern at this coverage. Interestingly, no LEED pattern is observed at higher energy (120 eV), suggesting that Mg atoms induce a long-range disorder (more than two or three layers). Note that RT could induce inter-diffusion phenomenon between Mg and Si atoms leading to an amorphous underlayer identified by XPS measurement in a previous study as Mg_2Si silicide ultrathin film.[14]

However, no other study has ever been made on this ultrathin silicide layer at RT, while in the 20–50 nm range, Mg_2Si silicide layers were extensively studied[19,27–30] for mechanical, electronic, and thermoelectric applications.

Figure 3(b) displays an empty state STM image recorded after 0.7 ML of deposition. Slightly below one monolayer, Mg deposit organizes itself as 2D flakes with a homogeneous height of approximately 4 Å, as shown on the corresponding height profile. These flakes exhibit an average lateral size between 10 and 50 nm and extend in a 2D growth mode, on top of the Mg underlayer previously formed.

Figure 3(c) shows an empty state STM image of the surface after 1 ML of Mg deposition. As coverage increases, the Mg flakes tend to densify to form a homogeneous ultrathin film. The non-continuous behavior of this layer is, however, not surprising at RT since many studies have reported the influence of annealing on the metallic deposit morphology. No noticeable size modifications are observed at this coverage; the Mg flakes still exhibit an average height of around 4 Å. This measure is consistent with the Mg atom diameter (2.9 Å) added to 70 pm, the height of the interface silicide layer. Figure 3(d) shows a filled state STM image of the surface obtained after the deposition of about 3 Mg MLs. A lateral size range of the Mg flakes between 10 nm and 50 nm is still observable, with a measured average height close to 1 nm which approximates with a factor of three times the measured thickness obtained after 1 ML of Mg deposition. We can suppose that every Mg flake belonging to a previous monolayer is used as a ground floor for the 2D growth of the flakes that as a consequence shapes the next one. Thus, the third monolayer probably grows on top of the previous two stacked layers in a layer-by-layer mechanism, leading to the formation of a homogeneous Mg film with low surface roughness.

Using scanning tunneling spectroscopy (STS), I(V) profiles were recorded at RT by collecting the tunnel current as a function of the tip-sample bias voltage over a ±5 V range. Scan areas of around 100 × 100 nm^2 were analyzed for clean silicon substrate and for 0.25 ML, 1 ML, and 3 ML Mg coverages.

From the shape of the I(V) curves plotted in Figure 4(a), we can observe I(V) features related to the electronic states of the different surfaces. In particular, both 1 Mg ML and 3 Mg ML curves exhibit a metallic behavior, in comparison to the semiconducting behavior obtained for both silicon substrate and the silicide underlayer.

A focus on these I(V) curves at low current is shown in Figure 4(b). The semiconductor behavior of the silicide layer is visible in Figure 4(c) with a gap of 0.74 eV. Note that for clean silicon surface, the maximum valence band is

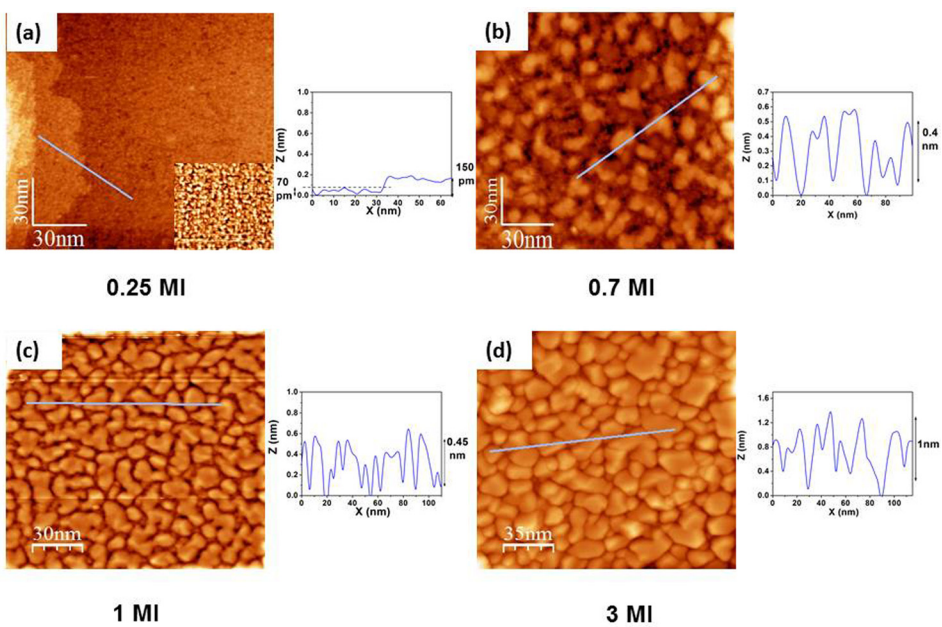

FIG. 3. Topographic STM images of the Mg deposit onto Si(100)-2 × 1 recorded for different coverages and corresponding height profiles. (a) 150 × 150 nm^2 empty state STM image after 0.25 ML of Mg deposition. (b) 150 × 150 nm^2 empty state STM image after 0.7 ML. (c) 150 × 150 nm^2 filled state STM image for 1 ML deposited. (d) 175 × 175 nm^2 filled state STM image after 3 deposited ML.

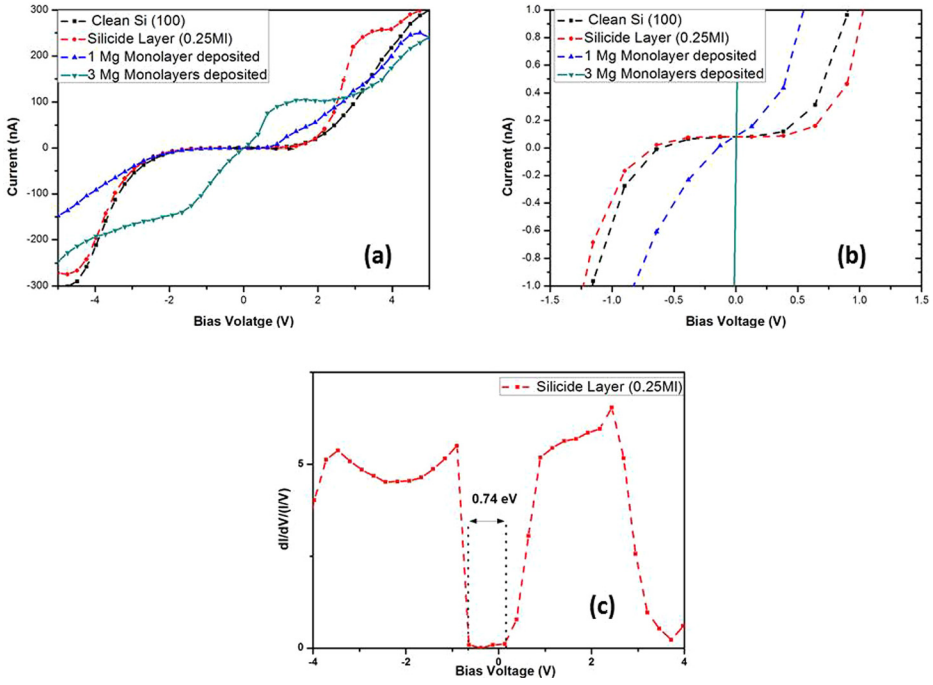

FIG. 4. (a) Average I(V) measurements monitored by STS on 100 $\times$ 100 nm^2 scan area for clean silicon and different Mg coverages. (b) Relevant focus on I(V) spectra presented in (a). (c) STS (dI/dV)/(I/V) characteristics for the silicide layer after 0.25 Mg monolayer deposited.

0.4 eV below the Fermi level, in agreement with an earlier report.[31] On the other hand, the characteristic I(V) behavior observed for 1 and 3 ML highlights the metallic nature of those Mg films grown on top of the ultrathin silicide underlayer. Figure 4(c) shows the (dI/dV)/(I/V) derivative curve from Figure 4(b), providing the local density of states[32,33] of silicide thin film with a band gap of 0.74 eV, in very good agreement with the previous measurements performed by several groups in the 10–50 nm range of Mg_2Si thin films.[27,29]

Figure 5 displays Auger peak-to-peak signals during *in-situ* oxidation process of one Mg monolayer. From theses curves, we clearly identify three different modes of oxygen adsorption. As expected in region (I), the Mg peak shifts totally to a lower energy from 45 to 35 eV due to oxidation of Mg. Oxygen peak linearly increases, while the intensity of the Mg peak at 45 eV drastically decreases (compared with initial intensity of Mg peak at 45 eV) as well as silicon. Note that there is no shift of the silicon Auger peak, indicating

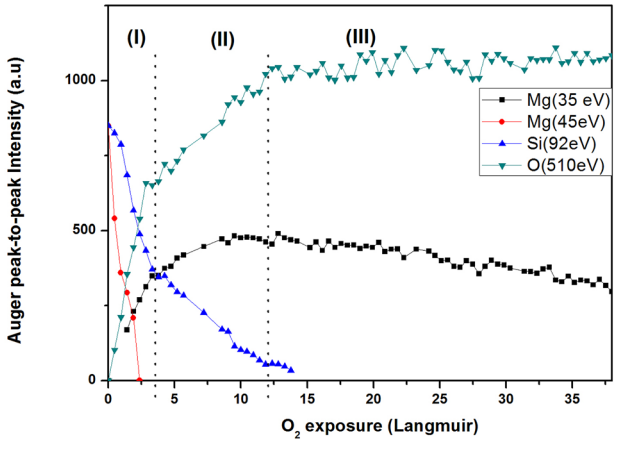

FIG. 5. Auger peak-to-peak signals of Mg, Si, and O as a function of O_2 exposures during *in-situ* oxidation process at RT ($P_{O2} = 1 \times 10^{-8}$ T) of one Mg monolayer.

that oxygen atoms cover the Mg monolayer with no oxidation of the silicon substrate which seems protected by the silicide interfacial layer and giving a remarkable Si/Mg_2Si/MgO stack, considering that MgO and Mg_2Si are such strongly bonded compounds. With increasing oxygen exposure, we clearly observe in region (II) that the kinetic of oxygen adsorption drastically changes with an obvious break followed by a slowdown of the oxygen adsorption. Concomitantly, the Mg oxidized signal (35 eV) increases while all the metallic Mg atoms (at 45 eV in region (I)) get oxidized. This behavior is explained by a decomposition of the interfacial silicide where buried Mg atoms move from the silicide layer towards the surface to form more Mg oxide. The reaction leading to partial decomposition of silicide and formation of magnesia at the surface were previously reported at higher temperature in thicker silicide layers.[30,34] This self-limited process is followed by a decrease of Mg oxide peak while oxygen atoms still incorporate on top of the surface in region (III).

Note that at the end of oxidation process, a thermal treatment at 500 °C enables to go back to the second obvious break, resulting in the desorption of oxygen atoms, adsorbed during regime (III).

In conclusion, both AES growth curves and topographic STM images recorded for wide range coverages show a different growth mode compared to RT deposition of metal on semiconductor that usually leads to the 3D growth mode.[35–37]

Growth mode of Mg on Si(100)-(2 $\times$ 1) at RT takes place in two successive steps. First, the formation of an ultrathin silicide layer occurs up to 0.25 deposited ML as previously suggested in XPS and STM studies and then identified from STM and STS-I(V) curves with a specific spectroscopic signature and a 0.74 eV electronic band gap. Thereafter, as Mg deposition increases, a layer-by-layer growth mode is set with metallic Mg atoms deposited on top of the formed silicide film. The ultrathin silicide layer acts as a reaction barrier at the interface preventing Si and Mg from coming into

contact and forming more silicide beyond 0.25 ML deposited, proved by STS with a metallic behavior of 1 and 3 Mg monolayers.

During RT oxidation process of one Mg monolayer, we have shown that the silicide layer prevents also the silicon oxidation. This indicates a potential role of Mg as an easily removable encapsulant for silicon, in analogy with the use of arsenic or selenium in the GaAs case.[38] With more oxygen exposure at RT, Mg atoms of the silicide layer diffuse to the surface to form more Mg oxide and probably improve significantly the quality of the MgO/silicon interface.

This work has been made possible thanks to the financial support of the following organizations: Région Provence-Alpes-Côte d'Azur (PACA), Institut Carnot STAR, and ville de Marseille. The authors thank B. Aufray, J.-Y. Hoarau, and H. Nguyen Thi for their generosity having contributed to optimize the experimental system dedicated to this study.

[1]D. A. Buchanan, IBM J. Res. Dev. **43**, 245 (1999).
[2]R. Jansen, Nat. Mater. **11**, 400 (2012).
[3]L. Yan, C. M. Lpoez, R. P. Shrestha, and E. A. Irene, Appl. Phys. Lett. **88**, 142901 (2006).
[4]C.-Y. Su, M. Frederickx, M. Menghini, L. Dillemans, R. Lieten, T. Smets, J. W. Seo, and J.-P. Locquet, Thin Solid Films **520**, 4508 (2012).
[5]S. Yuasa, T. Nagahama, A. Fukushima, Y. Suzuki, and K. Ando, Nat. Mater. **3**, 868 (2004).
[6]S. Vizzini, H. Oughaddou, J. Y. Hoarau, J. P. Bibérian, and B. Aufray, Appl. Phys. Lett. **95**, 173111 (2009).
[7]S. Vizzini, H. Oughaddou, J. Y. Hoarau, J. P. Biberian, M. Bertoglio, and B. Aufray, Appl. Phys. Lett. **103**, 261601 (2013).
[8]S. Vizzini, H. Oughaddou, C. Léandri, V. K. Lazarov, A. Kohn, K. Nguyen, C. Coudreau, J.-P. Bibérian, B. Ealet, J.-L. Lazzari, F. A. d'Avitaya, and B. Aufray, J. Cryst. Growth **305**, 26 (2007).
[9]H. Oughaddou, S. Vizzini, B. Aufray, B. Ealet, J.-M. Gay, J.-P. Biberian, and F. A. d'Avitaya, Appl. Surf. Sci. **252**, 4167 (2006).
[10]M. Kiguchi, S. Entani, and K. Saiki, Phys. Rev. B **68**, 115402 (2003).
[11]M. Mantilla, N. Jedrecy, R. Lazzari, and J. Jupille, Surf. Sci. **602**, 3089 (2008).
[12]P. Hutchison, M. M. R. Evans, and J. Nogami, Surf. Sci. **411**, 99–110 (1998).
[13]Y. Kawashima, H. Tanabe, T. Ikeda, H. Itoh, and T. Ichinokawa, Surf. Sci. **319**, 165–171 (1994).
[14]M. R. J. van Buuren, C. L. Griffiths, and H. van Kempen, Surf. Sci. **314**, 172 (1994).
[15]R. Shaltaf, E. Mete, and Ş. Ellialtioglu, Phys. Rev. B **69**, 125417 (2004).
[16]O. Kubo, A. Saranin, V. Zotov, T. Harada, T. Kobayashi, N. Yamaoka, J.-T. Ryu, M. Katayama, and K. Oura, Jpn, J. Appl. Phys., Part 1 **39**, 3740 (2000).
[17]J. D. Lavine, Surf. Sci. **34**, 90 (1973).
[18]J. Wilson and J. F. B. Hawkes, *Optoelectronics: an Introduction* (Prentice Hall, New York, 1983).
[19]I. Kogut and M.-C. Record, Thin Solid Films **522**, 149–158 (2012).
[20]A. Plecenik, L. Satrapinsky, P. Kús, S. Gazi, S. Benakca, I. Vávra, and I. Kostic, Physica C **363**, 224 (2001).
[21]W. H. Butler, X.-G. Zhang, T. C. Schulthess, and J. M. MacLaren, Phys. Rev. B **63**, 054416 (2001).
[22]S. Yuasa and D. D. Djayaprawira, J. Phys. D: Appl. Phys. **40**, R337 (2007).
[23]D. C. Jackson, T. E. Gallon, and A. Chambers, Surf. Sci. **36**, 381 (1973).
[24]F. C. Frank and J. H. Van der Merve, Proc. R. Soc. London, Ser. A **198**, 205 (1949).
[25]A. Barbier, Surf. Sci. **406**, 69 (1998).
[26]M. P. Seah, J. Phys. F: Met. Phys. **3**, 1538 (1973).
[27]A. Vantomme, G. Langouche, J. E. Mahan, and J. P. Becker, Microelectron. Eng. **50**, 237 (2000).
[28]S.-W. Song, K. A. Striebel, X. Song, and E. J. Cairns, J. Power Sources **119–121**, 110 (2003).
[29]M. R. J. van Buuren, F. Voermans, and H. van Kepen, J. Phys. Chem. **99**, 9519 (1995).
[30]Q. Xia, Q. XIe, X. Shen, J. Zang, Z. Yu, and K. Zhao, Appl. Surf. Sci. **257**, 7800 (2011).
[31]D. H. Rich, T. Miller, A. Samsavar, H. F. Lin, and T.-C. Chiang, Phys. Rev. B **37**, 10221 (1988).
[32]J. A. Stroscio, R. M. Feenstra, and A. P. Fein, Phys. Rev. Lett. **57**, 2579 (1986).
[33]R. M. Feenstra, J. A. Stroscio, and A. P. Fein, Surf. Sci. **181**, 295 (1987).
[34]N. Galkin, Thin Solid Films **515**, 8179 (2007).
[35]C. K. Shih, R. M. Feenstra, and P. Martensson, J. Vac. Sci. Technol., A **8**, 3379 (1990).
[36]B. M. Trafa, Y.-N. Yang, R. L. Siefert, and J. H. Weaver, Phys. Rev. B **43**, 14107 (1991).
[37]P. N. First, J. A. Stroscio, R. A. Dragoset, D. T. Pierce, and R. J. Celotta, Phys. Rev. Lett. **63**, 1416 (1989).
[38]C. Gonzalez, I. Benito, J. Ortega, L. Jurczyszyn, J. M. Blanco, R. Perez, F. Flores, T. U. Kampen, D. R. T. Zahn, and W. Braun, J. Phys.: Condens. Matter **16**, 2187–2206 (2004).